Korean J. Chem. Eng., 33(12), 3350-3358 (2016)
DOI: 10.1007/s11814-016-0228-x

pISSN: 0256-1115
eISSN: 1975-7220

Performance of polyacrylamide/Cr(III) gel polymer in oil recovery from heterogeneous porous media: An experimental study

Zahra Kargozarfard*, Masoud Riazi*,†, Shahab Ayatollahi, and Sheida Shahnazar*****

*Enhanced Oil Recovery (EOR) Research Centre, Department of Petroleum Engineering, School of Chemical and Petroleum Engineering, Shiraz University, Shiraz, Iran
**School of Chemical and Petroleum Engineering, Sharif University of Technology, Tehran, Iran
***Nanotechnology and Catalysis Research Centre (NANOCAT), University of Malaya, Kula Lumpur, Malaysia
(*Received 30 August 2015 • accepted 7 August 2016*)

Abstract−Water channeling due to reservoir heterogeneity is an important factor that could decrease the displacement efficiency of a water flooding process. In this study, the ability of polyacrylamide/ chromium acetate system on altering water path in heterogeneous layered media was investigated using glass bead micromodels. After the relevant parameters were optimized, a series of water and gel injection experiments were conducted in glass bead micromodel. The experimental results show that sweep efficiency is basically controlled by gel strength. The gel strength has a minor impact on the oil recovery from the higher permeable zone, whereas the oil recovery from the lower permeable zone is a strong function of gel strength. Gels with F and G strength codes were observed to divert the water path mostly into low permeable layers. Whereas, gels with B strength code or weaker would alter the water path within the higher permeable layers.

Keywords: Gel Polymers, Areal Sweep Efficiency, Micromodel, Water Production, Heterogeneity

INTRODUCTION

In the first stage of hydrocarbon recovery, hydrocarbon is produced as a result of reservoir natural energy. The natural energy of reservoirs usually recovers about 20% of hydrocarbon in place [1]; to produce the remaining and unrecovered oil, secondary recovery methods are applied. In the second stage of recovery, a fluid such as water or gas is injected into the reservoir to maintain the pressure. When the injected fluid is produced in considerable amounts from the production wells, the oil production will no longer be economical. Water flooding is the most widely used technique, which is applied in the second stage of oil production. The oil recovery of this process strongly depends on water sweep efficiency. Sweep efficiency is a measure of the effectiveness of oil displacement process that is determined based on the volume of the reservoir contacted by the injected fluid. Reservoir heterogeneity and high water mobility are known as two key parameters, which could decrease the displacement efficiency during water flooding process. During water flooding of heterogeneous and layered reservoirs, water breakthrough from high permeable layers occurs and low permeable zones are bypassed by the displacing fluid; consequently, significant amount of oil remains in the formation. This phenomenon is known as water channeling. If the swept high permeable zone is sealed, the injected fluid could shift to the previously bypassed low permeable zone. Hence the sweep efficiency and oil recovery improves.

Among different strategies for water production control, gel polymers are used as the most common method to overcome the associated problems. These Gel polymers initially were utilized to improve sweep efficiency during water flooding, and consequently to manage water shut-off [2]. Gel polymers are composed of a mixture of two components, including a water-soluble polymer and a crosslink agent. The main role of crosslink is to connect the polymer chains to generate a three-dimensional gel network. Generally, in the water shut-off process, the gelant is first injected into the formation, and once gel has formed the production from the well resumes [3,4]. The aim of choosing this process is placement of a stable gel in a preferred region to decrease the flow of produced water.

Extensive studies have been conducted in water control chemicals. In 1988, Zaitoun and Kohler showed that gels and polymers could selectively reduce effective water permeability more than the effective oil permeability [5]. This phenomenon is known as disproportional permeability reduction (DPR). In 1997, Barreau et al. performed several core-flooding experiments to investigate the impact of adsorbed polymer layer on relative permeability and capillary pressure in both water and oil wet cores. Their findings showed that, after polymer adsorption, residual water saturation increases in both cases during subsequent water flooding. Although the residual oil saturation was reported to increase in the oil wet core, however, it did not change the water wet one [6]. Liang and Seright investigated the mechanisms at which gel polymers decrease water's relative permeability more than that of oil [7]. They examined the validity of some assumptions through experimental studies, using polyacrylamide-chromium acetate system. Some of the proposed mechanisms are: Shrinking of gel in the presence of oil

†To whom correspondence should be addressed.
E-mail: mriazi@shirazu.ac.ir, mriazil80@gmail.com

[8], segregated oil and water pathway [7,9,10], wall effect [11] and the potential of gel to change the wettability of the media towards more water-wet [6]. They showed that the mechanisms would be different in different cases. They concluded that the multiple mechanisms could promote DPR; thus none of these mechanisms was mentioned as the only cause of this phenomenon. To visually investigate the flow behavior of water and oil in the presence of gel polymer, Al-Sharji et al. designed different transparent porous models [12]. Polyacrylamide-chromium acetate was utilized in these tests and the effective permeability to water and oil was estimated for different flow rates. The observations indicated that water flows through the gel in the pores, whereas oil pushes the gel in form of immiscible drops.

The majority of the previous works were performed in homogeneous systems to check the ability of different gel polymer systems in unequal permeability reduction. The effect of pertinent parameter on gelation time and gel stability has also been widely investigated [1,13-15]. However, the mechanisms of gel polymer treatment in heterogeneous systems need to be further investigated. Heshmati et al. experimentally investigated the polymer flooding in a heterogeneous micromodel [16]. In this study, a series of visualization experiments were designed on layered glass-bead micromodels, which was treated with gel-polymers. The objective of this study was to experimentally investigate the efficiency of chromium acetate/polyacrylamide on water cut reduction in a heterogeneous porous medium. The performance of this gel polymer on water shut-off was quantitatively and qualitatively analyzed by investigating the displacement efficiency of water flooding before and after the gelant injection stage. Partially hydrolyzed polyacrylamide (HPAM) is the most widely used water-soluble polymer, which has been successfully employed in enhanced oil recovery worldwide [17-20]. This paper not only gives a new understanding of the performance of gel systems, but also provides deeper knowledge on water and oil behavior in the presence of gel polymer through micromodel experiments. The pore scale mechanisms are discussed in detail as well. The results of this research can be helpful for better performing these gels for water shut-off in various complex reservoirs.

MATERIALS AND METHOD

1. Experimental Setup

Flooding tests were conducted using glass-bead micromodels to investigate the fluid flow behavior in porous medium. The transparent porous medium was prepared by sandwiching glass beads between two glass plates. The monolayer packing pattern was used to better observe the fluid flow through the models. The glass was already etched in acid solution to make them rough [21]. The heterogeneous models were composed of three layers with two different permeabilities: a high permeable layer between two low permeable layers. The diameter of glass beads used in the middle layer (high permeable) and the side layers (low permeable) was 840 μm and 210 μm, respectively. The allocated times for etching of each layer in the acid solution were proportioned to glass bead size; therefore, the depth of two sides layer was almost the same and less than that of the middle one. The properties of the model are shown in Table 1. Schematic view of the model is also shown in Fig. 1. The 3-D nature of these models and their random positioning would resemble the real water-flooded zones in layered and fractured formations. The distributers designed at the inlet and outlet would allow the flow to more equally enter the model. The distributer is designed to offer selective performance for the injected fluid. For example, during the primary water flooding, the distributer was completely filled with water, and when water reached to the end of the four branches of the distributer, water had the opportunity to enter each layer equally (two branches direct the flow into the high permeable layer; the other two branches are considered for the low permeable zone). In the models, the layers were set parallel to represent typical sedimentary layers.

Table 1. Properties of the micromodel used in this study

Area of low permeable layers (cm^2)	Area of high permeable layer (cm^2)	Porosity (%)	Pore volume (cm^3)
17.5	17.5	35.9	1.05

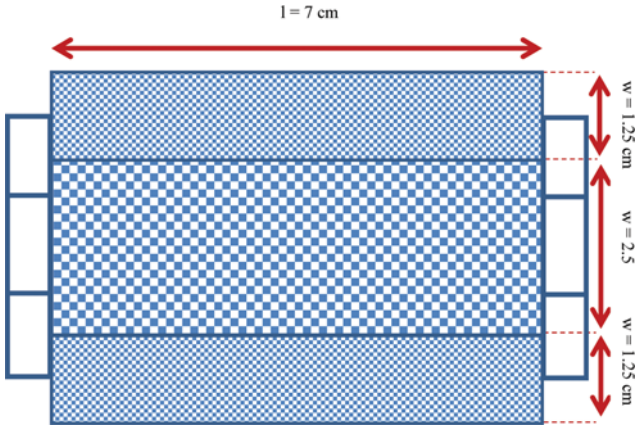

Fig. 1. Schematic of the micromodel used in this study.

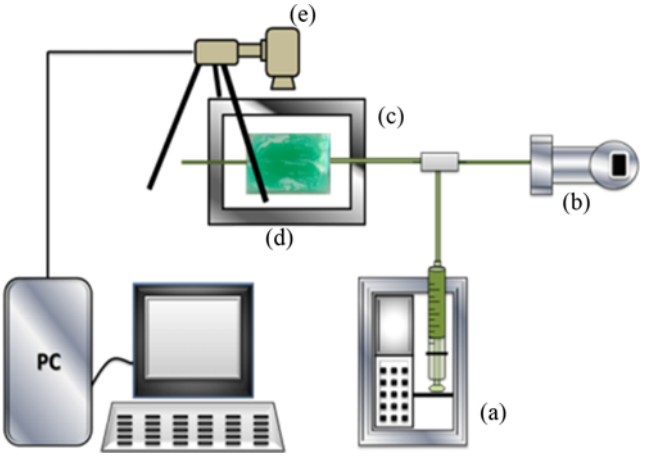

Fig. 2. Experimental setup.
(a) Syringe pump (c) Back light (e) Digital camera
(b) Differential pressure (d) Micromodel

Fig. 2 shows the experimental setup. In this setup, a syringe pump was used to inject fluids at constant flow rate. Digital camera was used to capture images. The differential pressure was used to monitor the pressure difference between the injected and produced phases.

2. Fluid System

Water soluble dye was used to have a color contrast between different phases within the model. For this purpose the volume ratio of dye to distilled water was selected as 1 : 10. The water phase has a density of 1.019 gr/cm^3 and viscosity of 1.0135 cP, at 25 °C and 1 bar.

A crude oil from an Iranian oil reservoir with a density of 0.854 gr/cm^3 and viscosity of 6.277 cP was used as the oil phase.

Partially hydrolyzed polyacrylamide (HPAM)-chromium (iii) acetate was utilized as gel polymer system in the experiments. The molecular weight of polymer was 5000000 and the degree of hydrolysis was 29%. The HPAM was purchased from Shahid Tondgoyan Petrochemical Co.

3. Experimental Procedure

3-1. Static Tests

All the tests were at ambient conditions. In the first step, a series of bottle tests were performed to check the properties of gel polymer system. A bottle test is a semiquantitative method to study gelation kinetic consisting of gelation rate and gel strength [22,23]. In this method, which was defined by Sydansk, gel strength was expressed as an alphabetic code of "A" through "I" [24]. According to this method, the gel sample in the bottle is inverted at different interval during development of gelation kinetic, and the code is assigned to them based on their ability to flow under the gravity force. Code "A" is attributed to a gel with the same viscosity as the original polymer solution, whereas "I" shows a rigid gel with no gel surface deformation by gravity [24].

For this purpose, the samples were prepared with different polymer concentration at ambient condition. The weight ratio of crosslinker to polymer concentration was selected 1 : 40 for all samples. The viscosity of the sample was estimated to be 7,500 cP. The corresponding code was allocated to these samples according to the Sydansk method (Table 2) [24].

Note that, to investigate the impact of dye added to water, two samples for all concentrations were prepared using distilled water and dyed water. It can be observed that gel strength increased with polymer concentration for both dyed and plain samples. However, the results showed that using the dyed water as a polymer solution solvent compared to plain water dramatically reduces the final gel strength code. The gel strength of the dyed sample initially increased with time, but the final gel strength (after 250 hours) became around "B" code. As indicated in Table 2, for the same polymer concentration, gel strength is lower in the dyed sample at the same time. According to these results, dye causes the gel network to be unstable. Hence, the gelant was prepared using distilled plain water for the flooding test to prevent the instability of the gel. Since the blue dyed water was used in the flooding experiments, the gel network strength might decrease due to diffusion of blue water in the gel network.

3-2. Flow Dynamic Tests

At the beginning, an experimental procedure was used to maintain the original oil in place at connate water saturation conditions and then followed by water flooding process. Some preliminary tests were performed to find an appropriate flow rate for water flooding stage of the main tests. The objective of this part was to monitor the effect of injection rate on the efficiency of water flooding, and consequently find the critical capillary number at which the water enters the high permeable zone. For this purpose, water was injected into the model, saturated with initial oil and irreducible water saturation conditions, at different flow rates.

After the flow rate was obtained, the designed experiments were at ambient conditions as the following procedure:

1. The pore volume of the model was measured by weighting method (Based on our calculation and the apparatuses used, the error of this test was about 10^{-3} ml.).
2. Saturating the model with dyed distilled water.
3. Oil was injected into the model to reach original oil in place at irreducible water saturation condition.
4. Primary water flooding was performed at constant flow rate until residual oil saturation was reached.
5. Gelant Injection was performed.
6. During the shut-in period, the inlet and outlet of model were sealed and the model was kept at ambient condition for the period of time.
7. Secondary water flooding process was performed, with the same flow rate as that of step 4.

The images of fluid distribution in the model were captured by

Table 2. Bottle tests for both plain and dyed water samples

Given time (hrs)	5,000 ppm		7,500 ppm		10,000 ppm		12,500 ppm		15,000 ppm	
	Dyed	Plain	Dyed	Plain	Dyed	Plain	Dyed	Plain	Dyed	Plain
38	A	B	B	B	B	C	C	D	C	E
62	B	B	B	C	B	C	D	E	D	E
97	A	B	B	C	C	C	D	E	D	E-F
127	A	B	B	C	C	C-D	D	E	D	F
151	A	B	B	C	C	D	C-D	F	D	F
176	A	B	B	C	C	D	C	F	C	F-G
200	A	B	B	C	B	D	C	F	C	G
223	A	B	B	C	B	D	C	F	B	G
250	A	B	A	C-D	B	E	B	F	B	G

Table 3. Experimental procedure of three different scenarios performed in this study

Test number	First water flooding flow rate (ml/hr)	Corresponding capillary number	PV of water injection in secondary water flooding	Gelant injection flow rate (ml/hr)	PV of gelant injection	Gelant injection side	Shut-in period (hrs)	Gel strength code	Second water flooding flow rate (ml/hr)
1	1.5	3.3×10^{-6}	1.10	0.05	0.268	Input	10	B	1.5
2	1.5	3.3×10^{-6}	1.01	0.05	0.268	Input	168	F	1.5
3	1.5	3.3×10^{-6}	0.94	0.05	0.268	Input	240	G	1.5

camera during the tests at specified time periods. The pressure drops of injected fluid at the same time periods were also recorded. Computer image processing technique was used to obtain the areal sweep efficiency at each condition. Table 3 shows the characteristics of the experiments performed in this study. Note that all gelant samples in the following table were prepared with the polymer concentration of 15,000 ppm.

As shown in Table 3, experiments performed in this study have the same injection flow rate for primary water flooding (1.5 ml/hr), gelant injection (0.05 ml/hr) and secondary water flooding (1.5 ml/hr); the only difference in these three scenarios is the shut-in period time, which directly affect the gel strength code.

Capillary number is the ratio between viscous and capillary forces. The corresponding capillary number was calculated using Eq. (1):

$$N_c=\mu u/\sigma \quad (1)$$

where, u is the Darcy velocity of the displacing phase (i.e., water). This is determined by dividing the water flow rate by cross sectional area of the micromodel open to fluid flow. σ is the interfacial tension (IFT) between water and oil phase and μ is the water viscosity. The capillary number, reported in Table 3, is estimated for primary water flooding. Hence, IFT between the dyed water and oil (i.e., 30 mN/m) was used.

Based on the capillary number, various flow regimes are expected to develop in the system. At field conditions capillary number varies between 10^{-6} and 10^{-4} [25].

3-3. Image Analysis

To study various recovery processes and examine transport mechanisms during miscible/immiscible displacements, micromodels are being widely used by researchers [26]. Glass micromodels are mainly used for qualitative analysis of the displacement processes in porous media. However, by utilizing image-analysis techniques, saturation of different phases could be quantified in glass micromodels. In this study, National Instruments Vision Assistant™ software was used to obtain required characteristic from captured images of the porous media. Vision Assistant, is an image analysis software that allows one to prototype application strategy quickly without need for programming.

Areal sweep efficiency (E_A) and oil recovery from each layer are two parameters for better evaluation of the efficiency of gel injection process. Areal sweep efficiency is defined by the ratio of area contacted by displacing agent divided by total area. In this study E_A are used to express areal sweep efficiency of water flooding. Thus, areal sweep efficiency in each stage was obtained by estimating the area occupied by the injected dyed water at that stage and the total area of the model. Oil recovery is reported as the percentage of original oil in place. To achieve this recovery, several parameters such as the volume of original oil in place, areal sweep efficiency of the injected water and average thickness of fluid (i.e., oil) in high permeable and low permeable layers should be identified. The volume of original oil in the micromodel was obtained from the injection time and the rate of oil injection. The average thickness was determined by "the volume of oil injected in the specified interval" and "the area of dyed water in the corresponding image," which was obtained from image process. For this purpose, oil is injected into the model which is saturated with dyed water. At the early stage of injection, oil enters into the high permeable layer; the thickness of fluid in this region can be easily estimated. By keeping injection, oil enters the low permeable zone and we have the advancement of oil front in both high and low permeable layers; for calculating the thickness of oil in low permeable region, the volume of oil in high permeable layer should be subtracted from the total volume of oil injection.

RESULTS AND DISCUSSION

In the initial test the range of flow rate was selected to be between 0.08-3 ml/hr, which corresponds to capillary number of 10^{-8}-10^{-6}. The objective of this study was to find the critical capillary number at which the water enters the high permeable zone. The flow rates of water injection used in the main experiments were determined based on these preliminary experiments.

As capillary number is defined as the ratio of viscous force to capillary force, the higher capillary number represents the case in which viscous force is dominant. Generally, low injection rate (10^{-8}-10^{-7} capillary number) results in the injected water to sweep the low permeable zones equally or even, at some cases, more than the high permeable zone. By increasing the flow rate (i.e., at capillary number of 10^{-6}), injected water significantly sweeps the high permeable zone. In our experiments, the injection rate at which water enters the high permeable zone was about 1.5 ml/hr. However, at low flow rates where the capillary number was low, the capillary force was dominant and the displacement mechanism would be controlled by spontaneous imbibition. During the injection of wetting phase, it covers the grain surface and occupy the smaller pores; thus non-wetting phase is bypassed in larger pores. Therefore, at low injection rates water sweeps the low permeable zones in addition to high permeable zone. When flow rate increases, viscous force become dominant and water enters the high permeable zone. At this condition, the high capillary zone (i.e.; low per-

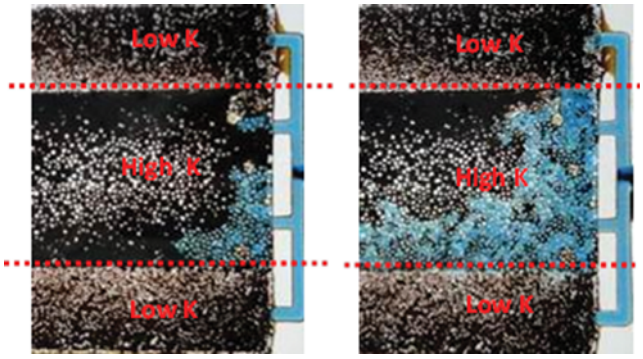

Fig. 3. Water flows into the high permeable layer after injection of: (a) 0.06 PV, (b) 0.12 PV.

meable zone) resists to high flow rate, and consequently hinders the injected fluid to enter this zone. Increasing the injection rate amplifies the viscous force to the extent from which it could overcome to the resistance of the low permeable zone. At this situation, the injected water sweeps the low permeable zone as well, by the mechanism of forced imbibition. The problem arises when the viscous force is dominant; however, not to the extent that the capillary force of low permeable zone to be overwhelmed. In this case a considerable amount of oil would remain in the medium.

According to the observation, the flow rate of 1.5 ml/hr was determined as the water flow rate for both primary and secondary water flooding stages.

In all the following images, the blue color represents the water phase and the brown color shows the oil phase. The areas covered by gelant are indicated by light blue.

1. Primary Water Flooding

In the current experiments the flow rate of injected water was set to 1.5 ml/hr. Under this flow rate, water significantly sweeps the high permeable zone and it cannot enter in the low permeable zone from the distributer (Fig. 3). This type of displacement would result in low oil recovery efficiency, early breakthrough and high water cut in heterogeneous porous media. Some techniques should be utilized to divert the injecting fluid into the unswept zones, in order to decrease water cut, consequently increasing the recovery efficiency.

2. Gelant Injection

After water injection, gelant was injected at the rate of 0.05 ml/hr. The gelant is first prepared in a beaker and then injected into the porous medium. The polymer solution and the crosslink solution are mixed with a fixed stirrer rate and at a specified temperature. That is, the gelant used in the model shows unique properties.

At the early stage of injection, gelant penetrated only into the high permeable zone but by continuing the injection some area of low permeable was also covered by gelant. In other words, in the early stage of gelant injection the front moved faster in high permeable zone (1.39×10^{-2} mm/s in high permeable layer compared with 2.13×10^{-3} mm/s in low permeable layer); however, over time the rate of advancement became equal in both zones (3.125×10^{-3} mm/s). As more gelant entered into the high permeable zone, the resistance to the flow into this zone increased. This caused the gelant to penetrate into the low permeable zone as well, with almost the same rate. This phenomenon is shown in Fig. 4 where the

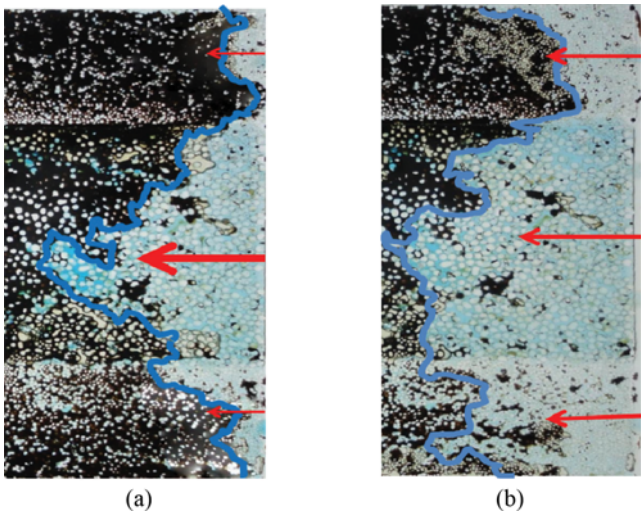

Fig. 4. Gelant advancement at: (a) Early stage of injection (b) by continuing the injection.

arrows with different lengths and thicknesses show the rate and amount of gelant advancement. In this figure the area covered by gel is highlighted by a blue border line. Observation showed that gelant tends to follow the water path compared to the paths saturated with oil. This could be due to the hydrophilic characteristic of gel. However, force balance in two different layers would mainly control the gelant flow path. These forces include the capillary forces in low permeable zone and the resistance of gel in high permeable zone. Resistance of gel is affected by the thickness of area occupied by gel and the gel strength, which depends on the time of gelant injection. Experimental results show that, contrary to water injection, reduction of gelant injection rate does not change the flow direction towards low permeable zone.

Another phenomenon observed, in this experiment, was fluid redistribution during the gelant injection. That is, oil displaced into larger pores and high permeable zone and a part of water moved into low permeable zone and smaller pores. Entering of gelant in low permeable zone caused oil production from this zone. After injection of 0.268 PV of gelant, injection was stopped and inlet and outlet of the model was sealed using Parafilm laboratory sealing film. Since the model had been kept at the ambient conditions for a limited period of time, sealing system can be assured. The evidence also confirms this point.

3. Shut-in Period

At this stage, the model was shut-in at the ambient temperature. Depending on the desired gel strength code, a different shut-in time period was allocated in each experiment. In this study, the effects of three gel strength codes on displacement process were investigated. Table 2 shows the shut-in time period of different experiments. Regardless of the shut-in time, gel swelling was observed in this period. Fig. 5 shows gel swelling in the low permeable zone of the model after ten days. The dashed line shows the position of the gelant front at the end of the gelant injection stage. This swelling occurs more likely due to water adsorption by the gel network. Polymeric gels are 3-D dimensional crosslinked networks and are able to absorb a high amount of their surrounding sol-

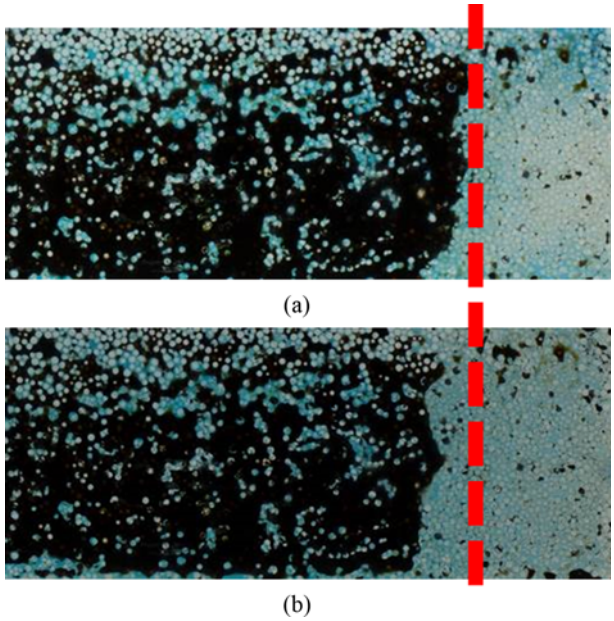

Fig. 5. Gel swelling in low permeable layer. (a) At the end of injection (b) after 7 days shut-in.

vents. This polymeric network is called "hydrogel" when the surrounding solution is water. The favorable property of these hydrogels is their ability to swell, when are kept in contact with an aqueous solution. That is, the contacted water with the hydrogel surface, penetrates into the polymeric network.

The obtained results show that fluid redistribution took place during shut-in period. Comparison of the images before and after shut-in reveals a little increase in the area covered by gel that can be one of the driving forces of fluid redistribution within the micromodel. This swelling contributes to some fluid redistribution within the model. Fig. 6 shows two sequential images of the same position. The highlighted oval part of the picture shows the changes in fluid distribution during shut-in period at the same position of high permeable zone.

4. Secondary Water Flooding

Finally, after reaching the designed gel strength code, secondary water flooding was performed with the same rate as the primary water flooding stage. As mentioned, the difference of three tests was in the strength code of the applied gel in the experiments.

In the first experiment, secondary water flooding was performed once the gel reached to B gel strength code. Gels with B strength code would change the water path within the higher permeable layer, and the remained oil of this layer was observed to be produced. Since the gel at this stage is flowing fluid, the gel acts similar to polymer. That is, it modifies the mobility ratio and recovers more oil from the high permeable zone. In this situation water cannot diffuse into the gel in both low permeable zones. However, gel is displaced in a piston-like form in low permeable zones during second water flooding. This stable front displacement causes a small oil displacement in low permeable regions.

In the second experiment, gel with code strength of F is not moving but is flexible. Although all layers were covered by gel, the water path was completely modified during the secondary water flooding. Water diffused through the gel network in all three layers, and a considerable part of oil, even in low permeable zone, was produced. Even though at this stage, water first diffused into the high permeable zone, after a short time, when it reached to the end of the distributer, it started entering into the low permeable zone. That is, due to the fact that as more gel is present in high permeable zone, the overall flow resistance in high permeable zone becomes greater than that of low permeable zone directing water to low permeable layers. At the end of this stage, the main part of the remaining oil in high permeable zone and a considerable part of oil in low permeable zone were produced. At the end of secondary water flooding stage, the trapped oil in low permeable zones was more than that in high permeable one. The result of this test shows that the presence of gel leads the displacing water into both low and high permeable zones. The interesting point that was observed is related to flow type of water and oil in gel; it was observed that water diffuses in gel. On the other hand, as Fig. 7 shows, the trapped oil in gel network is produced without any direct contact with the injected water, though they are in the form of non-continuous oil droplet. This type of production could be related to the elasticity properties of gel. The green circles in Fig. 7 highlight displacement of some trapped oil ganglia.

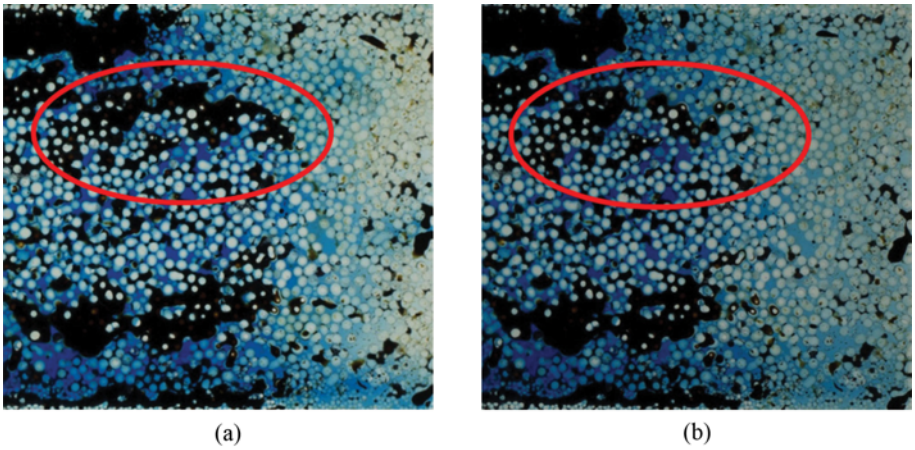

Fig. 6. Fluid distribution change in high permeable layer (Test. 2) (a) At the end of injection, (b) after 7 days shut-in.

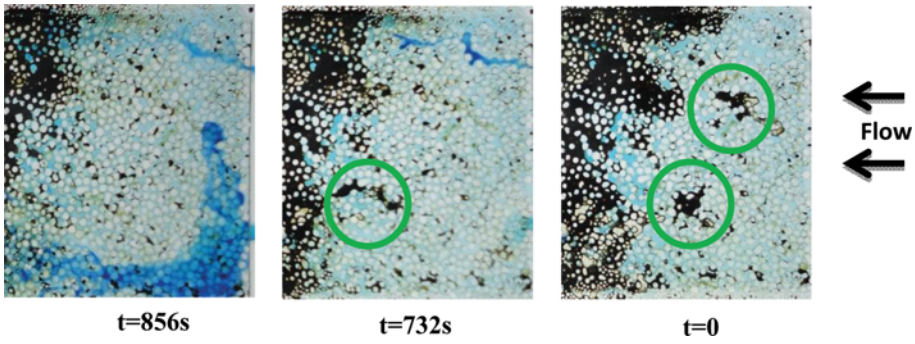

Fig. 7. Oil production due to gel elasticity during second water flooding stage in high permeable layer (Test. 2).

As the sequence of images shows, this displacement continues until the oil ganglia joins to the continuous oil film.

The third experiment performed used gel with G strength code.

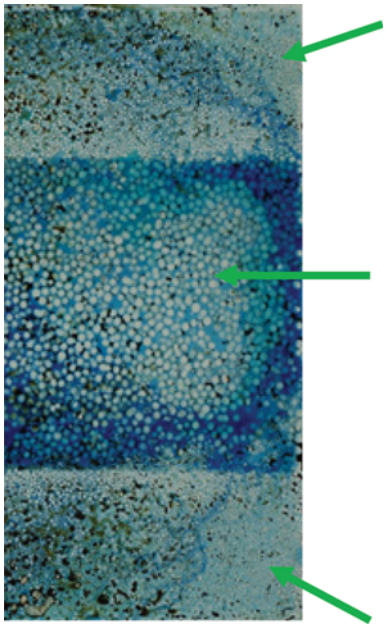

Fig. 8. Impermeable part of gel (Test. 3).

The results showed that this gel can change the path of water flow such that at the end of the second water flooding stage, all three layers were swept by water and considerable oil was produced from all layers. In this situation, injected water was able to diffuse in a limited area of gel and most of gel remained impermeable contrary to the previous test with F strength code, in which water could diffuse in almost all of the gel area. Furthermore, in the later test (case G) water entered in low permeable zone through flow between layers (Fig. 8); in fact, water selects the least resistant path to flow. In this test, oil production after water breakthrough was also detected, while in the previous cases (B and F) no oil production was observed from the low permeable zones after breakthrough from the high permeable layer.

Fig. 9 compares the areal sweep efficiency of injected water in primary and secondary water flooding for different gel strength codes. Note that the results of this study are based on the gel strength code. That is, all the gels with the same strength code are expected to show the same displacement efficiency. In fact, the possible relation between gel strength and its ability in altering water flow in a heterogeneous porous medium was investigated here, using the properties of gel at the bottle test and qualitatively assuming that porous media would change the properties in the same order of magnitude for each gel type.

As it can be seen from Fig. 9(a), areal sweep efficiency during primary water flooding sharply increases up to 0.8 PV of water flooding; however, E_A increases gradually after this point. No con-

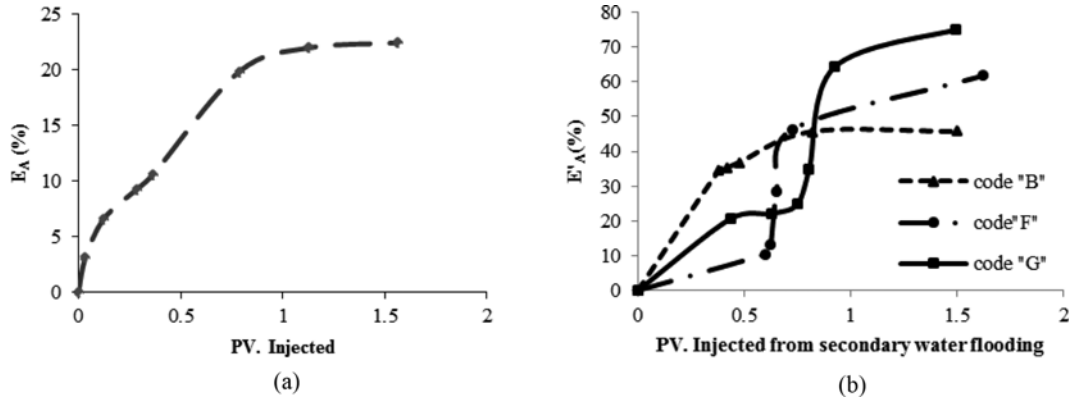

Fig. 9. Areal sweep efficiency of (a) primary water flooding, (b) secondary water flooding.

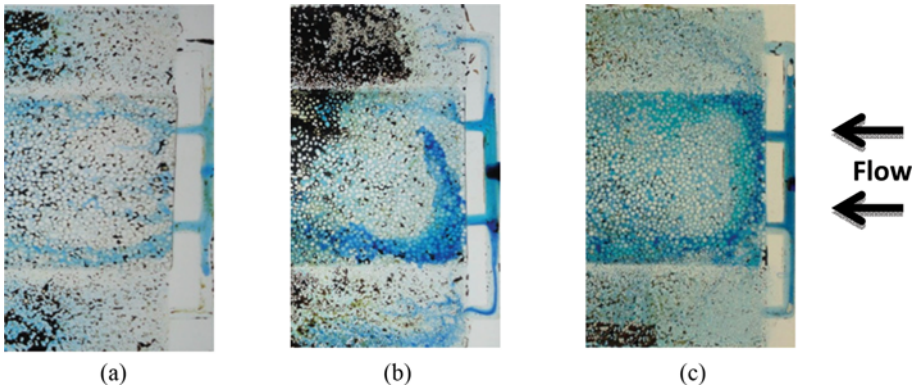

Fig. 10. Gel diffusion in different layers: (a) Code B, (b) Code F, (c) Code G.

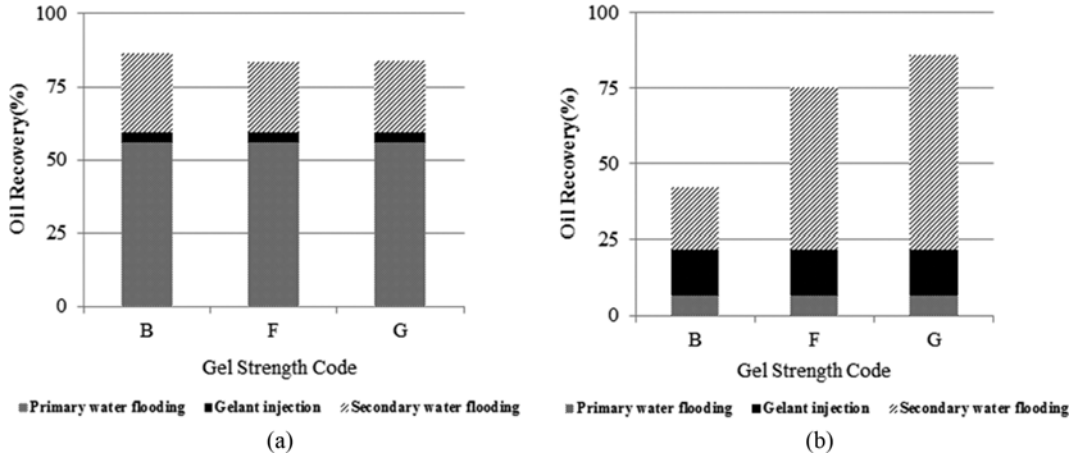

Fig. 11. Oil recovery of: (a) High K zone, (b) Low K zone.

siderable oil was produced after injection of 1.5 PV. Fig. 9(b) shows that during secondary water flooding, E_A increases for all three different gel codes. Flow of water in the gel network is strongly a function of gel strength code. If F gel strength code is used, water would enter into the low permeable zones after filling the distributer. The water penetration in gel with G strength code is almost similar to F strength code, with the only difference that water cross-flows in low permeable zone from layer boundaries. B gel strength code acts as polymer because of its lack of sufficient rigidity. It was observed that as gel with B strength code displaces within the media, a part of the residual oil is produced. Hence, the performance plot of secondary water flooding for this gel (code B) is similar to that of the primary water flooding. In this situation, the path of water only changes within the high permeable zone. The trend of the plots in the secondary water flooding is similar for both F and G gel codes. This trend is substantially different with that of primary water flooding. With these two kinds of gel, water can sweep the low permeable zones as well. The first section of this plot with sharp slope is related to the time that water passes the area covered by gel. At this stage, a considerable area of the model is swept by water. The remarkable point is that the areal sweep efficiency with G code is higher than that with F code in the interval of 0.2-0.5 PV. It could be due to less diffusivity power of G code compared to F code. As can be seen in Fig. 10(c), a significant area of the gel with G code is impermeable and water enters to the area free of gel after it diffuses in limited area of gel, whereas in F code (Fig. 10(b)) water passes through the porous medium after it diffuses in the area covered by gel. Finally, the areal sweep efficiency in G code becomes more than that of F code.

Fig. 11(a) and Fig. 11(b) compare the amount of produced oil at different flooding stages for different gel types in the high and low permeable zones, relatively. As can be seen from Fig. 11(a), (b) the main oil production from high permeable zone takes place during primary water flooding; however, in low permeable zone, the main oil recovery is due to the secondary water flooding. The results show that the gel strength has a minor impact on the oil recovery from the high permeable zone (Fig. 11(a)), whereas, the oil recovery from the low permeable zone is a strong function of gel strength. Thus, oil recovery increases in the low permeable zone as stronger gel is used.

A fraction of oil is recovered by gelant injection in low permeable zone due to water bypassing. As mentioned, oil displaced into larger pores and high permeable zone and a part of water moved into low permeable zone and smaller pores. That could be the main reason for higher recovery of low permeable zone in the gelant injection stage with comparison to the high permeable zone.

CONCLUSIONS

Efficiency of gel polymer injection in heterogeneous porous media is controlled by several factors. Gel strength code can play a vital role, although permeability differences between two layers and gel advancement in each layer are two other important parameters that should be considered in designing the process. The presence of gel with code strength of F in different zones helps water to enter in both high and low permeable zones due to affinity of this gel to water. Whereas, in the same situation, the gel with G strength code in low permeable zone has a lower capacity for water diffusion and water entrance in this zone occurs with different mechanisms. However, gels with B strength code would change the water path only within the higher permeable layer, when both high and low permeable layers are covered by this gel.

To sum up, the flow resistance difference of different zones determines whether or not water gets a chance to enter into different zones. As mentioned, this resistance is dependent on gel strength code, permeability difference of two layers and the gelant advancement in each zone.

Finally, the results of this study show that the improvement of sweep efficiency depends on gel strength. That is, the higher gel strength code results in higher sweep efficiency. The gel strength has a minor impact on the oil recovery from the higher permeable zone, whereas the oil recovery from the lower permeable zone is a strong function of gel strength.

NOMENCLATURE

E_A : areal sweep efficiency [%]
N_C : capillary number
u : darcy velocity [m/s]
μ : viscosity [kg/m·s]
σ : interfacial tension [N/m]

REFERENCES

1. A. M. Moghadam, M. V. Sefti, M. B. Salehi and H. Naderi, *Korean J. Chem. Eng.*, **31**, 532 (2014).
2. S. F. Bolandtaba and A. Skauge, *Transp. Porous. Med.*, **89**, 357 (2011).
3. H. A. Nasr-El-Din and K. C. Taylor, *J. Petroleum Sci. Eng.*, **48**, 141 (2005).
4. R. S. Seright, Improved methods for water shutoff, *Semmiannual Report*, 82 (1997).
5. A. Zaitoun and N. Kohler, Two-phase flow through porous media: Effect of an adsorbed polymer layer, *SPE Annual Technical Conference and Exhibition*, Society of Petroleum Engineers (1988).
6. P. Barreau, H. Berlin, D. Lasseux, P. Glenat and A. Zaitoun, *Spe. Reservoir. Eng.*, **12**, 234 (1997).
7. J. T. Liang, H. W. Sun and R. S. Seright, *Spe. Reservoir. Eng.*, **10**, 282 (1995).
8. R. A. Dawe and Y. Zhang, *J. Pet. Sci. Eng.*, **12**, 113 (1994).
9. S. Nilsson, A. Stavland and H. C. Jonsbraten, Mechanistic study of disproportionate permeability reduction, *SPE/DOE Improved Oil Recovery Symposium*, 1998 Copyright 1998, Society of Petroleum Engineers, Inc., Tulsa, Oklahoma (1998).
10. J. L. White, J. E. Goddard and H. M. Phillips, *J. Pet. Technol.*, **25**, 143 (1973).
11. A. Zaitoun, N. Kohler and M. A. Montemurro, Control of water influx in heavy-oil horizontal wells by polymer treatment, *SPE Annual Technical Conference and Exhibition*, 1992 Copyright 1992, Society of Petroleum Engineers Inc., Washington, D.C. (1992).
12. H. H. Al-Sharji, C. A. Grattoni, R. A. Dawe and R. W. Zimmerman, Pore-scale study of the flow of oil and water through polymer gels, *SPE Annual Technical Conference and Exhibition*, Society of Petroleum Engineers, Houston, Texas (1999).
13. T. Wan, W. Cheng, Z. Zhou, M. Xu, C. Zou and R. Li, *Korean J. Chem. Eng.*, **32**, 1434 (2015).
14. G. Sodeifian, R. Daroughegi and J. Aalaie, *Korean J. Chem. Eng.*, **32**, 2484 (2015).
15. F. Salimi, M. V. Sefti, K. Jarrahian, M. Rafipoor and S. S. Ghorashi, *Korean J. Chem. Eng.*, **31**, 986 (2014).
16. M. Heshmati, H. Mahdavi, M. Haghighi and M. Torabi, Visualization of polymer flooding in heterogeneous system using glass micromodels (2007).
17. C. Chelaru, I. Diaconu and I. Simionescu, *Polym. Bulletin*, **40**, 757 (1998).
18. W. Wang, Y. Liu and Y. Gu, *Colloid Polym. Sci.*, **281**, 1046 (2003).
19. J. C. Jung, K. Zhang, B. H. Chon and H. J. Choi, *J. Appl. Polym. Sci.*, **127**, 4833 (2013).
20. C. Mothé, D. Correia, F. de França and A. Riga, *J. Therm. Anal. Calorim.*, **85**, 31 (2006).
21. F. A. L. Dullien, Porous media fluid transport and pore structure, http://public.eblib.com/EBLPublic/PublicView.do?ptiID=1130068 (accessed).
22. H. Jia, W. F. Pu, J. Z. Zhao and F. Y. Jin, *Ind. Eng. Chem. Res.*, **49**, 9618 (2010).
23. M. Simjoo, M. Vafaie Sefti, A. Dadvand Koohi, R. Hasheminasab and V. Sajadian, *Iran J. Chem. Chem. Eng.*, **26**, 99 (2007).
24. R. D. Sydansk and P. Argabright, United States Patent Patent (1987).
25. J.-R. a. A. B. Z. Ursin, *Fundamentals of petroleum reservoir engineering* (1997).
26. F. Vermolen, J. Bruining and C. Van Duijn, *Transp. Porous. Med.*, **44**, 247 (2001).